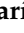








Article

Raman Spectroscopic and Sensory Evaluation of Cocoa Liquor Prepared with Ecuadorian Cocoa Beans Treated with Gamma Irradiation or Induced Electromagnetic Field Fermentation

Tania María Guzmán-Armenteros ¹, Jenny Ruales ¹, Cristina Cuesta-Plúa ², Juan Bravo ², Marco Sinche ³, Edwin Vera ¹, Edison Vera ³, Paul Vargas-Jentzsch ³, Valerian Ciobotă ⁴, Fernando E. Ortega-Ojeda ^{5,6}, Andrés Proaño ⁷, Armando Echeverría ⁸ and Luis Ramos-Guerrero ^{9,*}

¹ Departamento de Ciencia de Alimentos y Biotecnología, Facultad de Ingeniería Química y Agroindustria, Escuela Politécnica Nacional (EPN), Quito 170525, Ecuador; tania.guzman@epn.edu.ec (T.M.G.-A.); jenny.ruales@epn.edu.ec (J.R.); edwin.vera@epn.edu.ec (E.V.)

² Agencia de Regulación y Control Fito y Zoonosanitario (AGROCALIDAD), Av. Interoceánica km 14 1/2, Tumbaco 170184, Ecuador; maria.cuesta@agrocalidad.gob.ec (C.C.-P.); juanitob920@hotmail.com (J.B.)

³ Departamento de Ciencias Nucleares, Facultad de Ingeniería Química y Agroindustria, Escuela Politécnica Nacional, Ladrón de Guevara E11-253, Quito 170525, Ecuador; marco.sinche@epn.edu.ec (M.S.); edison.vera@epn.edu.ec (E.V.); paul.vargas@epn.edu.ec (P.V.-J.)

⁴ Rigaku Analytical Devices, Inc., 30 Upton Drive, Suite 2, Wilmington, MA 01887, USA; valerian.ciobota@rigaku.com

⁵ Departamento de Ciencias de la Computación, Universidad de Alcalá, Ctra. Madrid-Barcelona Km. 33.6, 28871 Alcalá de Henares, Madrid, Spain; fernando.ortega@uah.es

⁶ Instituto Universitario de Investigación en Ciencias Policiales (IUICP), Universidad de Alcalá, Libreros 27, 28801 Alcalá de Henares, Madrid, Spain

⁷ Programa de Reactivación de Café y Cacao, Ministerio de Agricultura y Ganadería, Av. Eloy Alfaro y Av. Amazonas, Quito 170518, Ecuador; carlos.proaño@rikolto.org

⁸ Facultad de Ciencias Técnicas, Universidad Internacional del Ecuador, Quito 170411, Ecuador; neecheverriall@uide.edu.ec

⁹ Grupo de Investigación Bio-Quimioinformática, Carrera de Ingeniería Agroindustrial, Facultad de Ingeniería y Ciencias Aplicadas, Universidad de Las Américas (UDLA), Quito 170503, Ecuador

* Correspondence: luis.ramos.guerrero@udla.edu.ec; Tel.: +593-098-054-8444



Citation: Guzmán-Armenteros, T.M.; Ruales, J.; Cuesta-Plúa, C.; Bravo, J.; Sinche, M.; Vera, E.; Vera, E.; Vargas-Jentzsch, P.; Ciobotă, V.; Ortega-Ojeda, F.E.; et al. Raman Spectroscopic and Sensory Evaluation of Cocoa Liquor Prepared with Ecuadorian Cocoa Beans Treated with Gamma Irradiation or Induced Electromagnetic Field Fermentation. *Foods* **2023**, *12*, 3924. <https://doi.org/10.3390/foods12213924>

Academic Editor: Ksenija Radotić

Received: 29 August 2023

Revised: 19 September 2023

Accepted: 26 September 2023

Published: 26 October 2023



Copyright: © 2023 by the authors. Licensee MDPI, Basel, Switzerland. This article is an open access article distributed under the terms and conditions of the Creative Commons Attribution (CC BY) license (<https://creativecommons.org/licenses/by/4.0/>).

Abstract: Cocoa liquor is the primary precursor of the worldwide highly appreciated commodity chocolate. Its quality depends on several factors, such as the type of cocoa, the fermentation process, and the control of the contaminants in the fermented beans. This study aims to evaluate whether the induced magnetic field treatment during the fermentation process or the pathogen reduction with gamma irradiation after the fermentation affect the characteristics of the cocoa liquor obtained from Ecuadorian cocoa beans. For this purpose, liquor samples from controls (standard process), from beans treated with an induced magnetic field up to 80 mT, and from beans irradiated with nominal doses up to 3 kGy were characterized through Raman spectroscopic analysis and sensorial evaluation. The most relevant bands of the cocoa liquor were assigned according to reports from the literature, spectroscopic data, and chemometrics. The spectra corresponding to different treatments and doses were visually very similar, but they could be discriminated using OPLS-DA models, where the most intense Raman signals were attributed to the lipid components. The sensorial evaluation rated the presence of floral, fruity, almondy, acid, and bitter flavors, along with astringency and intense aroma, and these attributes exhibited variable behavior depending on the dose of the irradiation or magnetic treatment. Therefore, both treatments may exert an influence on cocoa beans and, therefore, on the cocoa liquor quality.

Keywords: chocolate; cocoa beans; cocoa liquor; Raman spectroscopy; magnetic field; fermentation

1. Introduction

The production of cocoa beans and the chocolate industry constitute an essential share of the economy of many countries. Moreover, there has been an increase in consumers' interest in premium chocolates containing organic, single-origin, and Fairtrade cocoa, as well as chocolates with high cocoa contents [1].

Chocolate is a mixture of cocoa liquor, sweeteners, emulsifiers, and other ingredients suspended in cocoa butter or other alternative fat sources [2], subjected to refining, conching, tempering, and standardization [3]. The cocoa fermentation process hugely influences the quality of the chocolate; during this step, the beans go through chemical and physical transformations that define desired characteristics such as aroma and flavor [4]. Cocoa fermentation occurs due to the sequential microbial action of yeasts, lactic acid bacteria and, eventually, acetic acid bacteria [5]. Each group of microorganisms produces specific compounds responsible for the cocoa beans' sensory and organoleptic attributes. For instance, volatile organic compounds (such as fatty acid ethyl esters and acetate esters) are produced through the action of yeasts involved in reactions of the amino acid metabolism during the fermentation. These esters are responsible for the development of the chocolate's aromas and flavors characterized by fruity notes [6].

The application of electromagnetic fields can help to improve the fermentation processes of different agricultural products [7], including cocoa beans [8]. This is considered to be a safe technology that does not generate toxic products and is not difficult to apply. Food processes induced by electromagnetic fields have shown effectiveness in terms of bacterial activation, stimulation of their growth, production of metabolites, and improved sensory quality when compared to conventional treatments [9].

On the other hand, consuming chocolate with a high cocoa content has positive effects on health [10], such as lowering blood pressure, inhibiting platelet activation, improving endothelial function, and avoiding insulin resistance [11]. However, these benefits may be overshadowed in chocolate by a microbial attack by, for instance, aerobic psychrotrophic microbes, spores from thermophilic acidophilus, or mesophilic aerobic bacteria [12]; hence, the importance of applying treatments that hamper microorganisms' growth.

Gamma irradiation has been applied for decades to eliminate food's microbiological risks (i.e., pathogenic and food-spoilage microorganisms) without compromising nutritional properties, consumer safety, and sensory quality [13]. In this technology, food products are exposed to the ionizing radiation emitted by cobalt-60 or cesium-137 radioisotopes, which have high energy and a penetration capacity of several feet [14]. Additional applications of irradiation of food materials include shelf-life extension, delaying ripening in fresh products [15], sprout inhibition in bulbs and tubers, insect disinfecting in cereals, pathogen elimination or reduction in animal products and vegetables [16], and improving food's mycotoxicological safety [17]. Food irradiation, also known as ionization, exhibits exciting benefits such as the absence of chemical residues after the treatment, the avoidance of important temperature increases during the process, versatility since it can be applied to low- and high-moisture products as well as fresh or frozen food [18], and easiness regarding the operation of the irradiators, since the gamma rays are emitted in all directions continuously and at a predictable rate [19]. Moreover, the process does not require much electric energy, and it is not a water-consuming method. However, gamma rays are unsuitable for some products, like plums and pears, in which quality properties are affected by the reduction in firmness [20]. The dose sensitivity of a product depends on its composition, because some macromolecules are more susceptible to radiation than others (lipids > carbohydrates > proteins). In this sense, radiation is widely recommended for fish, meat, and poultry. Conversely, fruits and vegetables are characterized by higher contents of carbohydrates that could experience hydrolysis reactions, while foods with high lipid contents are susceptible to auto-oxidation [21]. Therefore, the dose must be carefully selected depending on the nutritional profile of the product.

Food exposed to a proper irradiation dose for technical purposes is safe and nutritionally adequate according to international experts [22]. The flavor and some nutritional

properties could undergo modifications, but these changes are generally less noticeable than those observed when applying conventional preservation treatments (e.g., cooking, canning, pickling, freezing, and drying) [17]. Additionally, food ionization could be more expensive than other methods, the availability of irradiation facilities is limited, and certain importing markets decline irradiated products [23]. Nevertheless, the unit costs can be lowered if larger volumes of product are subjected to this treatment, and if irradiation facilities operate close to their maximum capacity. In addition, many products have overcome trade barriers through gamma irradiation [24]. Many people still resist accepting irradiated food due to misconceptions about ionizing radiation. In these cases, consumer reliance on this technology could be acquired through education and scientific evidence. All things considered, gamma treatments exhibit a more significant number of advantages than drawbacks. The key challenge of this food technology is to identify the dose at which the desirable aspects are maximized while shortcomings are minimized.

Another critical subject of concern, in addition to the fermentation process under induced magnetic fields and microbial safety, is that chocolate quality depends on the raw material quality and the manufacturing steps [25]. Physical, chemical, and sensory methods are used to analyze the chocolate quality. Safety, color, aroma, flow behavior, and texture are the principal quality parameters in chocolate [26]. In addition, other quality attributes that are assayed in chocolates include particle size distribution, viscosity, melting profile, and hardness [27], sensory properties related to mouthfeel [28], and fat, protein, carbohydrate, water, and ash contents [29].

At the same time, there is an increasing requirement for quick, objective, and accurate techniques to inspect the quality of foods like chocolate [30]. In this respect, spectroscopic tools (e.g., Raman, IR, etc.) are fast, simple, and inexpensive; they do not require much sample preparation, cause almost no sample destruction, and do not need reagents that later constitute chemical waste [31,32]. In this regard, Raman spectroscopy has a wide range of potential usages in food quality assessment, including the detection of components in the food matrix such as macromolecules (e.g., protein, carbohydrates, fat, etc.), migration of packaging material to the product, the presence of synthetic dyes and carotenoids, determination of changes experienced during stages of manufacture at a structural or conformational level, and the detection and evaluation of counterfeits and adulterations, sample structure, type, molecular conformation, crystallinity, and microorganisms, among many other factors [33–35].

In this regard, this study aims to evaluate whether the cocoa bean fermentation process performed under an induced magnetic field and the gamma irradiation of naturally fermented cocoa beans could cause changes in the quality of their respective cocoa liquors. For this purpose, spectroscopic measurements were carried out on cocoa liquor samples from regularly fermented and non-irradiated beans (control), from irradiated beans (up to 3 kGy), and from beans fermented under electromagnetic field treatments (up to 80 mT). At the same time, the impact of gamma irradiation on the sensory profile was also analyzed through a sensory evaluation carried out on non-irradiated and irradiated samples.

2. Materials and Methods

2.1. Cocoa Bean Fermentation under Induced Magnetic Fields

The CCN-51 cocoa (*Theobroma cacao* L.) pods were obtained from local producers in Santo Domingo de los Tsáchilas in Ecuador. The pods did not have defects or damage, and they had a uniform orange color (an indicator of their degree of maturity). The obtained grains were duly packed in polyethylene bags, transported, and stored (7–12 °C for less than 32 h) in a cold room until the tests. The cocoa pods were washed and opened manually to obtain clean grains without impurities or defects. For each assay, a total of 3 kg of ready-to-ferment slime beans was placed in 5 L plastic fermentation boxes with ventral and lateral openings. The incubation system temperature (37 ± 0.5 °C) and humidity ($85 \pm 0.8\%$) were controlled and maintained (B 5042, Heraeus, Hanau, Germany) throughout the fermentation process. The fermentation was stopped after seven days, and

the beans were then dried in a forced-air rotary kiln (R610 Roller, Rotary Kiln, Nove, Italy) at 60 °C for 4 h to pass to the next step, as described in Section 2.3.

Subsequently, 24 h after starting the fermentation process, the samples were subjected to a second mild fermentation (in an aerobic phase) under low-frequency magnetic fields of 0 (control), 5, 48, 62, and 80 mT, using a Helmholtz prototype for electromagnetic emissions. The prototype consisted of a designed and validated Helmholtz coil with an area of 0.2 m, an alternating current generator, and a digital signal connection system (to control the uniformity of the oscillating magnetic field (OMF) between the coils). The setup and operation details are available in a previous report [8].

2.2. Gamma Irradiation Treatment of Fermented Cocoa Beans

The regularly fermented and dried cocoa beans from the National and CCN-51 varieties were maintained at room temperature (18 °C). The cocoa beans (1.3 kg) were packed in polystyrene trays covered with a plastic film, placed vertically, and then irradiated at nominal doses from 0.10 to 3.00 kGy in triplicate (Tables S1 and S2). They were irradiated in a Co-60 panoramic irradiator (Laboratorio de Tecnología de Radiaciones, Escuela Politécnica Nacional, Quito, Ecuador). Non-irradiated samples of each variety were used as controls for the experiment. The dosimetry was assessed by four pellet alanine dosimeters, Batch E2044562 (Bruker BioSpin, Quito, Ecuador), placed in one of the replicates at different tray positions (Figures S1 and S2). The exposed dosimeters were read using an electron paramagnetic resonance spectrometer (e-scan, Bruker BioSpin, Billerica, MA, USA) [36].

2.3. Cocoa Liquor Samples

The liquor samples were prepared from CCN-51 cocoa beans via the fermentation process under induced magnetic fields (0, 5, 48, 62, or 80 mT), and from CCN-51 and National cocoa beans after being fermented and irradiated (0.10, 0.20, 0.30, 0.45, 0.60, 0.75, 1.00, 2.00, and 3.00 kGy nominal doses only for sensorial treatment). The cocoa liquor was prepared by an in-house traditional method; for instance, 200 cocoa beans were toasted at 123 °C for 10 min in an oven (UF30, Memmert, Schwabach, Germany). Then, the beans were manually peeled and pre-grinded (KN 295, Foss, Hillerød, Denmark) for 2 min at room temperature (25 °C). The ground beans were refined (502, NCM, Taipei, Taiwan) for 15 min. The obtained cocoa liquor was poured into casts, cooled at 15 °C, and stored in labeled plastic bags at 0 °C once the liquor was solidified.

2.4. Raman Spectral Measurements of Cocoa Liquor Samples

Raman measurements of the cocoa liquor samples were performed using a spectrometer (BD_Progeny_LT, Rigaku Raman Technologies, The Woodlands, TX, USA) with a 1064 nm Nd:YAG laser source and a Peltier-cooled InGaAs photodiode array. The temperature was controlled with a cryogenically cooled Ge detector to ensure the solid state of the samples. The measurement conditions were 490 mW, 1000 ms of exposure, and 5 counts. The measurements were taken randomly at different spots on the sample's surface, and each sample had 20 replicates. Before the Raman measurements, a daily calibration method was carried out with a benzonitrile standard.

2.5. Sensorial Evaluation of Cocoa Liquor from Gamma-Irradiated Cocoa Beans

Six trained panelists assessed the sensory profile of the liquors corresponding to the irradiated CCN-51 and National cocoa beans, using a quality rating method. The following attributes were considered: floral, fruity, almondy or nutty, cocoa, acid, bitter, and astringent flavors, as well as aroma intenseness. The parameters were rated in duplicate, with an intensity scale from 0 to 5 (0 = absence; 1 = very mild; 2 = mild; 3 = medium; 4 = strong; 5 = very strong). The average ambient conditions of the testing/sensory room were 25 ± 2 °C and 56% relative humidity. The sensory evaluation was performed similarly to a previously reported method [37] for liquor samples, with some modifications.

A portion of the liquor was placed on the tongue's surface to identify and quantify the attributes of interest. The panelists rinsed their mouths with water to remove the remaining flavors and waited 5 min before testing another sample. The cocoa liquors were tested in a solid state, at room temperature.

2.6. Multivariate Data Analysis of the Raman Spectra of Cocoa Liquor

The Raman spectra were imported in bulk using a script (steps' sequence) in Origin v2021 9.8 (OriginLab Corporation, Northampton, MA, USA). The spectra were moved and organized sequentially in Excel (Microsoft Corporation, Redmond, USA) and then transposed to have the objects (observations, subjects, or items) in rows and the wavelengths (variables) in columns. Then, the required demographic, categorical, and qualitative variables were added to describe the different samples, groups, categories, or classes.

A few spectra were plotted randomly to identify the spectral zone corresponding to the region of interest (ROI). The rest of the ranges (without information) were removed from the data. The spectral ROI of all samples was then treated with a well-known preprocessing sequence commonly used within spectroscopy. The sequence consisted of a baseline correction, SNV standardization (subtracting the arithmetic mean and dividing by the standard deviation), and soft smoothing (noise reduction) using the Savitzky–Golay method. Finally, the multivariate data analysis was performed using the orthogonal partial least squares regression with discriminant analysis (OPLS-DA) in SIMCA (Sartorius, Göttingen, Germany). This analysis was performed in a procedure that seeks the most significant possible separation between samples.

3. Results and Discussion

3.1. Cocoa Liquor Raman Spectra

Figure 1 shows the average Raman spectra of 20 cocoa liquor samples prepared with the CCN-51 variety. Table 1 shows the frequency assignment for the samples shown in Figure 1.

The main constituents of cocoa liquor are lipids, since around 44% of its precursor (cocoa beans) corresponds to this type of molecules [38]. Triacylglycerols (TAGs) account for around 98% of the cocoa lipids, and their composition differs based on geographical origin [39]. Cocoa butter is formed mainly by three TAGs: glycerol-1-palmitate-2-oleate-3-stearate (POS), glycerol-1,3-distearate-2-oleate (SOS), and glycerol-1,3-dipalmitate-2-oleate (POP) [40]. Palmitic (C16:0), stearic (C18:0), oleic (C18:1) [41,42], and linoleic (C18:2) acids [43] are the main components of the TAG cocoa butter fatty acid profile. In this sense, the Raman spectra of the cocoa liquor should also be mainly represented by the spectral signals of those compounds. Indeed, the Raman spectra of cocoa liquor exhibit more intense bands at 1071, 1301, and 1445 cm^{-1} , which occur at similar wavelengths found in fatty acid moieties reported previously in the literature, corresponding to the C–C stretching, C–H twisting, and scissoring deformation modes, respectively [44]. Accordingly, the Raman measurements conducted in cocoa butter showed bands regarding the form-V polymorphs at 1063 and 1297 assigned to the stretching $\nu(\text{C–C})$ and skeletal and $\tau(\text{CH}_2)$ twisting modes, respectively [45]. Also, the Raman peaks in several TAGs (i.e., tripalmitin, trimyristin, trilaurin, triundecanin, and triacetin) showed strong bands due to the CH_2 scissoring vibration at 1445 cm^{-1} [46,47]. Therefore, the mentioned bands of cocoa liquor can be assigned confidently to fatty acid groups and alkanoyl moieties of the cocoa triacylglycerols.

Additionally, it should be noted that most of the Raman bands occurring in lipid materials are ascribed to the acyl chain, which is why the fatty acid spectra are similar to the TAG spectra containing them [48]. Hence, the following bands have been reported: between 1050 and 1150 cm^{-1} , corresponding to $\nu(\text{C–C})$ stretching, at 1296 cm^{-1} for $\delta(\text{CH}_2)$ twisting, and between 1400 and 1500 cm^{-1} for $\delta(\text{CH}_3)$ or $\delta(\text{CH}_2)$ deformations [49]. The literature has indicated that monosaturated and unsaturated fatty acids show peaks occurring at the same wavenumbers, with the difference that the latter have broader bands.

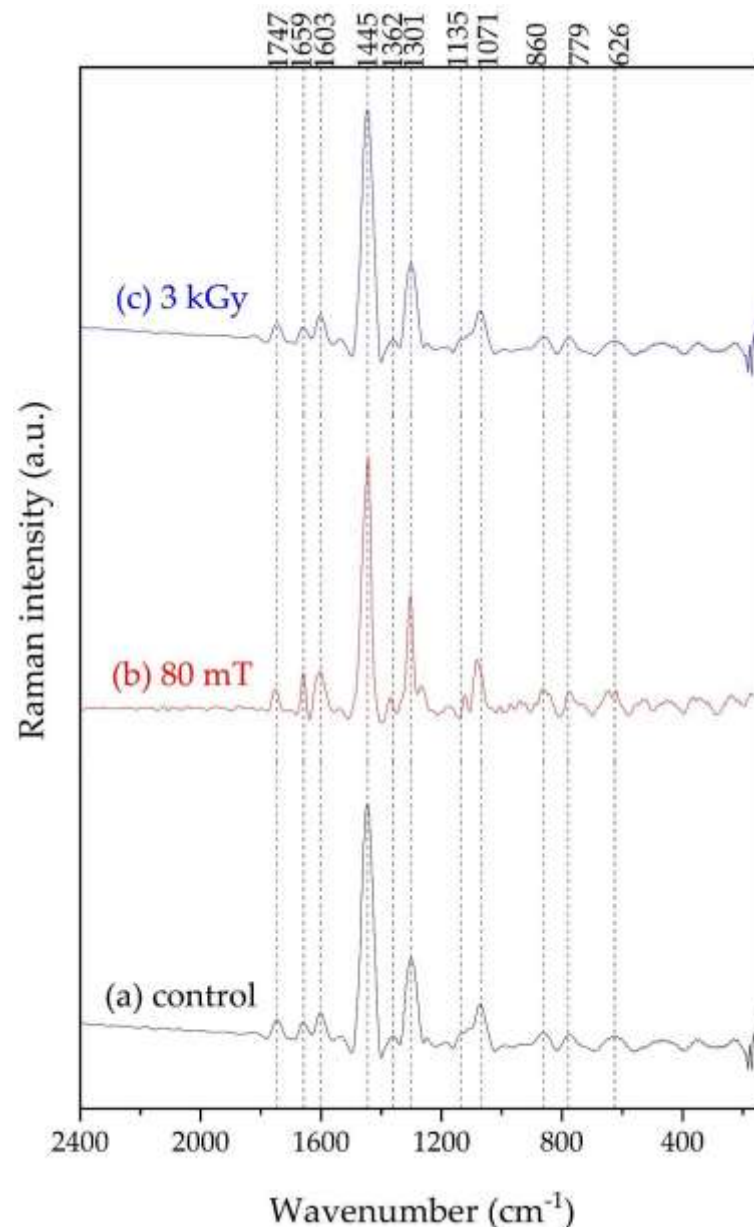


Figure 1. Average Raman spectrum of the cocoa liquor from the CCN-51 variety: (a) standard process (control); (b) fermentation process under induced magnetic field (80 mT); (c) gamma irradiation process (3 kGy).

Other Raman signals occurring in the assessed cocoa liquor spectra and related to the fatty acid fractions include the band at 1664 cm^{-1} , which can be assigned to the stretching of the C=C double bonds, and the band at 1747 cm^{-1} , which is related to the elongation of the C=O belonging to the ester carbonyl stretching mode [44]. Both spectral features in the spectrum of cocoa liquor seem to be typical of unsaturated fatty components, particularly the oleic acid moiety (1659 and 1744 cm^{-1}) [50]. Therefore, these bands could be attributed to the oleic acid moiety from the cocoa liquor. However, the presence of other TAGs cannot be ruled out, because the signals reported previously for other TAGs are very close (1743 cm^{-1} for tripalmitin, and 1742 cm^{-1} for trimyristin and trilaurin) [51].

The previous assignment of the C=O and C=C double bonds is consistent with another work on cocoa butter that depicted peaks at 1745.4 and 1733.8 cm^{-1} , representing the crystallization forms III and IV, respectively [52]. These forms correspond to the region described for the stretching vibrations due to C=O bonds. Likewise, the C=C stretching

region exhibits a band at 1662.7 cm^{-1} , associated with the presence of oleic acid and representative of form-IV crystallization in cocoa butter at room temperature [52]. In addition, the literature on Raman spectra reports their corresponding monoacid triglyceride assignments of C=O stretching vibrations at $1720\text{--}1750\text{ cm}^{-1}$, C=C stretching vibrations at $1600\text{--}1680\text{ cm}^{-1}$, CH₂ or CH₃ group scissoring deformations at $1400\text{--}1500\text{ cm}^{-1}$, CH₂ twisting at approx. 1300 cm^{-1} , and C–C stretching vibrations in the $1060\text{--}1090$ and $1110\text{--}1180\text{ cm}^{-1}$ regions [48].

Although most of the predominant Raman features in the cocoa liquor spectra correspond to the fatty components, peaks from other compounds present in cocoa liquor may appear. Nonetheless, some signals that were previously assigned to the fatty fraction may overlap with others corresponding to lignin, cellulose, hemicellulose, pectins, phenolic compounds, and alkaloids, which are present in cocoa liquor in lower amounts. In this regard, the weak signals corresponding to lignin may occur in cocoa liquor's Raman spectra. This is why a previous work reported values of the lipid–lignin ratio in the cocoa nibs [32]. The lignin features observed in the spectra that could correspond to this component appeared at $356, 456, 539, 626, 779, 1135, 1220, 1301, 1362, 1445, 1603,$ and 1659 cm^{-1} . Consistently, the bands at similar wavelengths in the native lignin spectra have been identified at $357, 463, 537, 634, 787, 1134, 1216, 1297, 1454, 1602,$ and 1658 cm^{-1} [53].

Most of the strongest cellulose bands may not be visible in the cocoa liquor samples due to the overlap of more intense ones corresponding to other compounds; for instance, the reported cellulose and hemicellulose bands are expected to overlap with those of the monolignol units of lignin [54]. However, some weak signals appear in the spectra at $356, 456, 989, 1071, 1108, 1250, 1301, 1362,$ and 1445 cm^{-1} , which are similar to those reported for softwood cellulose at $351, 458, 1073,$ and 1298 cm^{-1} [55]. Another study found similar wavelengths for some bands occurring in cellulose I from bacterial origin [56] and *Valonia ventricosa*'s cellulose [57]. It distinguished bands at 366 and 462 (assignment not reported), 997 and 1071 (assigned to C–O stretching ring modes), 1249 (assignment not reported), 1293 (CH₂ twisting), 1359 (C–H deformation), and 1454 (O–H deformation) cm^{-1} [57]. Considering that hemicellulose has similar chemical bonds to cellulose, their bands could be overlapped [53].

Pectins are plant cell wall polysaccharides that are formed by D-galacturonic acid [58]. The polygalacturonic (pectic) acid spectra depicted bands at $537, 621,$ and 775 (ring “brezing”), 853 (C6–C5–O5–C1–O1), 990 (γ (COOH)dimers), 1079 (ν (CO) + δ (OH)), 1105 (ν (CC)(CO)), 1145 (ν (COC) glycosidic bond, ring), 1254 (δ (CH)), and 1740 cm^{-1} (ν (C=O)COOH) [59]. The cocoa liquor spectra showed bands in similar locations to those previously reported at $539, 626, 779, 860, 989, 1071, 1108, 1135, 1250,$ and 1747 cm^{-1} .

Regarding polyphenolic compounds, cocoa and chocolate have great contents of procyanidin flavonoids, catechin, and epicatechin [60]. Cocoa liquor may show some Raman features that support their presence, as discussed below based on the occurring peaks reported in the literature. Examples of these compounds include the aromatic ring vibrations from 1300 to 1600 cm^{-1} , C–C ring vibrations from 1500 to 1600 cm^{-1} due to the stretching vibration of the two opposite benzene ring quadrants and the simultaneous contraction of other quadrants, and the bending in the C–H plane. Moreover, the bands at 1400 to 1500 cm^{-1} are due to the C–C ring vibrations originating from the stretching of the ring's semicircle, the contraction of other rings, and the simultaneous CH bending [61,62]. In this sense, the band observed at 1603 cm^{-1} in the spectra could be linked to the vibrations originating from the aromatic ring ν (C=C) of the polyphenolic compounds [63].

Table 1. Experimental frequencies (cm^{-1}) and assignment of the Raman spectra for the Ecuadorian cocoa liquor (CCN-51 variety).

| Experimental Wavenumber (cm^{-1}) | Intensity | Assignment Vibrational Modes | Proposed Compound | Reported Wavenumber (cm^{-1}) | Reference |
|--|-----------|--|--|--|-----------|
| 626 | VW | Skeletal deformation of aromatic rings, substituent groups, and side chains | Native lignin | 634 | [53] |
| | | - | Polygalacturonic (pectic) acid H-Pec | 621 | [59] |
| | | C=C-C deformation | Theobromine | 626 | [50] |
| | | OH out-of-plane deformation/ $\nu(\text{C}=\text{C})$ ring | Ascorbic acid | 621 | [71,72] |
| 779 | VW | Skeletal deformation of aromatic rings, substituent groups, and side chains | Native lignin | 787 | [53] |
| | | Ring “brezing” | Polygalacturonic (pectic) acid H-Pec | 775 | [59] |
| | | O=C-C deformation [68] | Theobromine | 777 [69] | [68,69] |
| 860 | VW | (C6-C5-O5-C1-O1) | Polygalacturonic (pectic) acid H-Pec (a-glycosidic bonds in H-Pec) | 853 | [59] |
| | | N=C-H deformation | Caffeine | 850 | [68] |
| 1071 | M | $\nu(\text{C}-\text{C})$ | C-C in cocoa butter | 1000–1150 | [44] |
| | | $\nu(\text{C}-\text{C})$ | Cocoa butter polymorphs form V | 1063 | [45] |
| | | $\nu(\text{C}-\text{O})$ ring modes | Cell wall of <i>Valonia ventricosa</i> cellulose | 1071 | [57] |
| | | $\nu(\text{CO}) + \delta(\text{OH})$ | Polygalacturonic (pectic) acid H-Pec | 1079 | [59] |
| | | $\nu_s(\text{C}-\text{N})$ | Caffeine | 1080 | [68] |
| | | $\nu(\text{C}-\text{O}-\text{C})$ and $\delta(\text{C}-\text{O}-\text{H})$ | Ascorbic acid | 1081 | [71,72] |
| 1135 | sh | A mode of coniferaldehyde unit | Native lignin | 1134 | [53] |
| | | $\nu(\text{COC})$ glycosidic bond, ring | Polygalacturonic (pectic) acid H-Pec | 1145 | [59] |
| | | $\nu(\text{C}-\text{N})$ | Caffeine | 1131 | [68] |
| 1301 | S | $\tau(\text{CH}_2)$ | Cocoa butter polymorphs form V | 1297 | [45] |
| | | $\tau(\text{C}-\text{H})$ | C-H in cocoa butter | 1200–1400 | [44] |
| | | Aryl-O of aryl-OH and aryl-O-CH ₃ and C=C stretching of coniferyl alcohol units | Native lignin | 1297 | [53] |
| | | $\delta(\text{HCC})$ and $\delta(\text{HCO})$ | Softwood cellulose | 1298 | [55] |
| | | $\tau(\text{CH}_2)$ | Cell wall of <i>Valonia ventricosa</i> cellulose | 1293 | [57] |
| | | $\nu(\text{C}-\text{N}) + \rho(\text{CH}_3)$ | Theobromine | 1298 | [69] |
| | | $\nu(\text{C}-\text{N})$ | Theobromine | 1296 | [50,68] |
| | | $\nu(\text{C}=\text{N}) + \nu(\text{C}-\text{N})$ | Theobromine | 1360 | [69] |
| 1362 | VW | C-H deformation | Cell wall of <i>Valonia ventricosa</i> cellulose | 1359 | [57] |
| | | $w(\text{CH}_2)$, $\delta(\text{C}-\text{O}-\text{H})$ | Ascorbic acid | 1371 | [71,72] |

Table 1. Cont.

| Experimental Wavenumber (cm ⁻¹) | Intensity | Assignment Vibrational Modes | Proposed Compound | Reported Wavenumber (cm ⁻¹) | Reference |
|---|-----------|---|--|---|-----------|
| 1445 | VS | $\delta(\text{C-H})$ | C-H in cocoa butter TAGs: tripalmitin, trimyristin, trilaurin, triundecanin, and triacetin | 1400–1500 | [44] |
| | | $\delta(\text{C-H})$ | | 1445 | [46,47] |
| | | Guaiacyl ring vibration | Native lignin | 1454 | [53] |
| | | O-H deformation | Cell wall of <i>Valonia ventricosa</i> cellulose | 1454 | [57] |
| | | $\delta(\text{CH})$, CH ₂ scissoring | Ascorbic acid | 1452 | [71,72] |
| 1603 | W | Symmetric aryl-ring stretching | Native lignin | 1602 | [53] |
| | | $\nu(\text{C=C})$ | Aromatic ring from polyphenolic compounds | max. 1613 | [63] |
| | | $\nu(\text{C=C}) + \nu(\text{C-N}) + \delta(\text{CH}_3)$ | Theobromine | 1594 | [69] |
| | | $\nu(\text{C=C})$ | Caffeine | 1600 | [68] |
| 1659 | VW | $\nu(\text{C=C})$ | Cocoa butter region attributed to the olefinic band | 1600–1700 | [44] |
| | | Ring-conjugated $\nu(\text{C=C})$ of coniferaldehyde | Native lignin | 1658 | [53] |
| | | $\nu_{as}(\text{C=O})$ | Theobromine | 1660 | [68] |
| | | $\nu_{as}(\text{C=O})$ | Caffeine | 1656 | [68] |
| | | $\nu(\text{C=C})$ ring stretching | Ascorbic acid | 1661 | [71,72] |
| 1747 | VW | $\nu(\text{C=O})$ | C=O in cocoa butter | 1700–1800 | [44] |
| | | $\nu(\text{C=O})\text{COOH}$ | Polygalacturonic (pectic) acid H-Pec | 1740 | [59] |

ν : stretching; ν_{as} : asymmetric stretching; ν_s : symmetric stretching; δ : bending; w : wagging; τ : twisting.

Methylxanthines are the most abundant alkaloids in cocoa, especially theobromine, caffeine, and theophylline; together with polyphenols, they are responsible for the beans' characteristic bitter taste [64–66]. The molecular structure similarities are shown in their Raman features, mainly in the 900 to 3200 cm⁻¹ range [67]. Nonetheless, the representative bands associated with alkaloids that were observed in the cocoa liquor spectra will be discussed next, even though most of them might be overlapped with others with more intense features. The theobromine spectra depicted bands at 460, 620, 777, 946, 1298, 1360, 1594, and 1660 cm⁻¹ [68,69]. Similar bands with slight shifts that corroborated the presence of this alkaloid in the analyzed samples were observed at 456, 626, 779, 940, 1301, 1362, 1603, and 1659 cm⁻¹; these could be assigned to $\delta(\text{pyrimidine ring}) + \delta(\text{CNO}) + \delta(\text{CH})$ [69], C=C–C deformation [50], O=C–C deformation, $\rho(\text{CH}_3)$, $\nu(\text{C-N}) + \rho(\text{CH}_3)$, $\nu(\text{C=N}) + \nu(\text{C-N})$, $\nu(\text{C=C}) + \nu(\text{C-N}) + \delta(\text{CH}_3)$, and C=O asymmetric stretching [68,69], respectively. Consistently, a study conducted on cocoa beans and their extracts reported some of the aforementioned Raman bands at 459, 620, 776, 1296, and 1594 cm⁻¹ and suggested that they constitute useful information to distinguish theobromine from theophylline [50,68]. All bands above 1000 cm⁻¹ may be overlapped with more intense ones, like those reported above. The Raman spectra of caffeine depict bands at 225, 850, 975, 1080, 1131, 1188, 1241, 1600, 1656, and 700 cm⁻¹ [68], while the cocoa liquor spectra of our study showed similar bands with slight shifts; this corroborates the presence of the aforementioned alkaloid in the analyzed samples. The bands at 225, 860, 1071, 1135, 1250, and 1699 cm⁻¹ found in cocoa liquor may be assigned to N–C–N deformation, N=C–H deformation, C–N symmetric stretching, C–N stretching, C–N stretching, and C=N stretching, respectively [68]. Also, the

bands observed at 1178, 1603, and 1659 cm^{-1} may be attributed to the C–C stretching, C=C stretching, and asymmetric C=O vibrations, respectively [68].

The presence of organic acids in Ecuadorian cocoa liquor has also been evidenced elsewhere [70]. The Raman spectra for ascorbic acid show bands at 452 (C–O in-plane deformation), 621 (OH out-of-plane deformation/C=C ring stretching), 984 (C–H and O–H bending), 1081 (C–O–C stretching and C–O–H bending), 1113 (C–O–C stretching), 1258 (C–O–H bending/twisting), 1371 (CH_2 wagging, C–O–H bending), 1452 (CH bending, CH_2 scissoring), and 1661 (C=C ring stretching) cm^{-1} [71,72]. The citric acid features may be present in the evaluated cocoa liquor spectra at 456, 626, 989, 1071, 1108, 1250, 1362, 1445, and 1659 cm^{-1} .

On the other hand, Figure 2a shows a 3D scatterplot of the scores for the cocoa liquor produced using fermentation under low-intensity induced magnetic fields. At first glance, the data were rather scattered, especially for the samples that received large magnetic field doses (Figure 2; front location in the front view, or right-hand location in the top view). Although the lab conditions were as controlled as possible during the processing of the cocoa liquor, such data dispersion was probably due to the many variables involved in this experimental (non-commercial) processing. Despite that, the figure shows a clear discrimination of the samples with respect to the different magnetic field treatments that they received. It should be noted that the points corresponding to the largest magnetic field doses tend to be the most separate from one another. This indicates that those samples were different in their Raman responses—that is, in their composition and possible properties. Figure 2b shows the contribution plot for the t0 samples (lower part) with respect to the t4 samples (upper part) shown in Figure 2a. This plot shows the variables explaining why the t0 samples deviate from the t4 samples. The intensity of the deviation is shown as lines. This way, the larger the line values (on the Y axis), the greater the variable's importance, and the sign of the line sequence (down = minus; up = plus) indicates the direction in which the variables deviate. The variables colored in orange are outside the three standard deviations (std dev) limit range; this means that they are even more important variables.

Figure 3a shows the 3D scatterplot of the scores for the cocoa liquor produced after the irradiation of the CCN-51 cocoa bean samples. These data were less scattered when compared to the set in Figure 2. The figure shows very good discrimination of the samples with respect to the different irradiation doses that they received, especially when the doses were higher. The front view (Figure 3a, left) shows that the samples treated with lower doses (darker blue dots) remained rather close to one another, which would indicate that those samples were less different from one another. This, in turn, would imply that their Raman responses were still similar at the macro scale, which suggests that their composition and possibly their properties were also somehow similar at the macro scale. On the other hand, the two largest doses (yellow and red dots on the right in Figure 3a, respectively) were completely separated from the rest of the samples and one another. This indicates that those samples were very different in their Raman responses and, thus, in their composition, and surely in their properties. Figure 3b shows the contribution plot for the non-irradiated samples (lower part) with respect to the 2.0 kGy irradiated samples (upper part), shown as the darkest blue and yellow dots in Figure 3, respectively. This plot shows the variables explaining why the non-irradiated samples deviate from the 2.0 kGy irradiated samples.

3.2. Sensory Attributes of the Cocoa Liquor from the Gamma-Irradiated Cocoa Beans

Table S3 and Figure 4 show the averages of the evaluated attributes in the cocoa liquor prepared from the irradiated beans of the CCN-51 and National varieties.

There are several odor-active compounds that enable humans to perceive the characteristic chocolate flavor [73]. Cocoa presents basic flavors like acid, bitter, astringent, sweet, and salty, as well as specific flavors such as cocoa, floral, fruity, and nutty. Chocolatiers appreciate and look for attributes such as floral, cocoa, sweet, and nutty, since they give chocolate special notes [74].

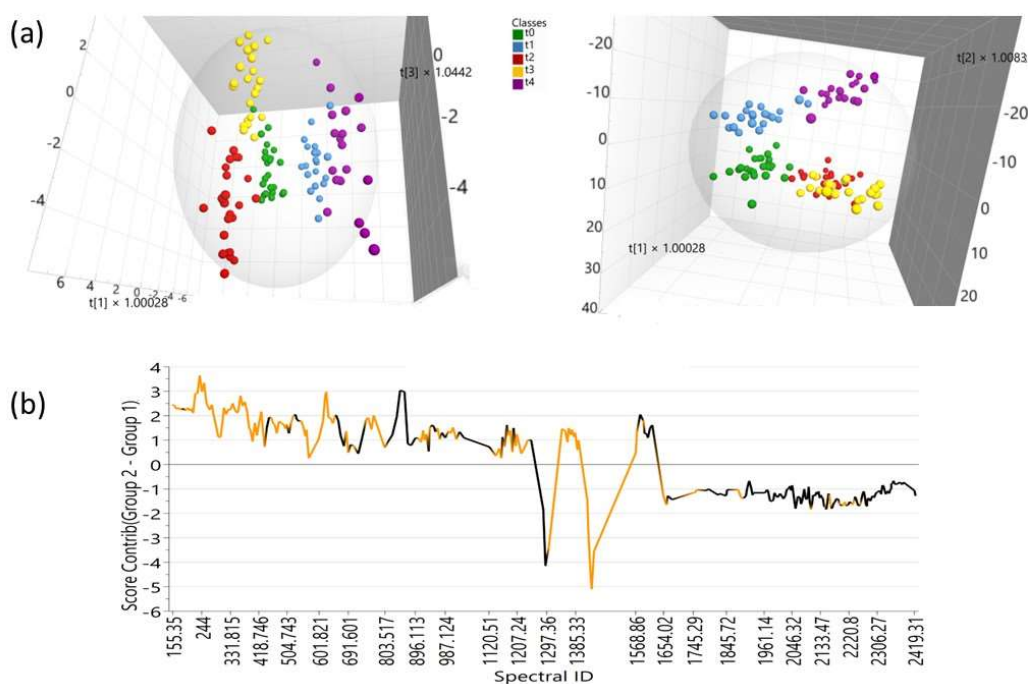


Figure 2. Chemometric analysis of the cocoa liquor produced using fermentation under induced magnetic fields: (a) Front and top (right-wise rotated) views of the 3D scatterplot for the scores. The magnetic field is shown as t0 (0 mT), t1 (5 mT), t2 (48 mT), t3 (62 mT), and t4 (80 mT). (b) Contribution plot for the t0 samples (lower/positive side) with respect to the t4 samples (upper/negative side). The orange-colored variables are outside the 3 std dev limit range.

The sensory attributes fruity, almondy or nutty, bitter, and astringent flavors, as well as the aroma intenseness, exhibited a very mild intensity in the CCN-51 control sample. Additionally, the floral attribute was absent, while cocoa and acid flavors showed a mild intensity. On the other hand, the National liquor control sample exhibited a medium intensity in the cocoa attribute and a mild intensity in the almondy or nutty flavor. Also, the fruity and floral attributes were absent, whereas the acid, bitter, and astringent flavors and the aroma intenseness showed a very mild intensity. The National variety showed higher values for the almondy, cocoa, and astringent flavors, as well as for the aroma intenseness.

Interestingly, the evaluated attributes in both cocoa varieties exhibited several changes in the irradiated samples. The very mild fruity attribute of the CCN-51 variety increased at 2.0 and 3.0 kGy. Therefore, it can be inferred that radiation could enhance the compounds responsible for the perception of this attribute, which was found in the fine varieties but minimal in the CCN-51 type. For example, β -myrcene and β -cis-ocimene are compounds attributed to the fruity flavor and floral aroma, respectively. β -Myrcene ($5.70 \pm 1.00\%$) and β -cis-ocimene ($5.20 \pm 0.70\%$) are present in the pulp of the fine cocoa variety SCA6, whereas the CCN-51 variety has less than 0.30% of these terpenes [75]. Other volatile compounds that have been found in CCN-51 include 2,3-butanediol, which is related to aroma, and acetophenone and 1-phenyl-2-ethanol, which are linked to fruity and floral notes [76]. The fruity and floral attributes associated with the National cocoa variety were enhanced by the irradiation, since it made them more evident to the senses. This may be akin to the enhancement in ethyl ethanoate (fruit fragrance) in rice wine achieved with the increase in the radiation dose [77].

The almondy flavor in CCN-51 was maintained with irradiation at doses up to 0.75 kGy, while at higher doses it experienced a progressive decrease. In the National variety, this flavor decreased non-uniformly with ionization at different doses, except at 0.45 kGy, where the initial value was maintained. There was a complete loss of the almondy attribute at 2.0 and 3.0 kGy in both varieties. Concerning the cocoa attribute in CCN-51, it diminished at all doses except at 0.20 kGy, where the mild intensity remained similar to the

control, while the greatest loss occurred at 1.0 kGy. In the National samples, this attribute also decreased, reaching the lowest values at 0.3, 2.0, and 3.0 kGy. In cocoa and chocolate, pyrazines, aldehydes, and esters are related to the nutty, cocoa aroma, and fruity flavors, respectively. Several aroma-active compounds identified in a cocoa liquor study included tetramethylpyrazine, benzaldehyde, and 3,5-diethyl-2-methylpyrazine, which confer nutty, almondy, and cocoa aromas, respectively [78]. Thus, we can infer an influence of radiation on the compounds responsible for the aforementioned attributes.

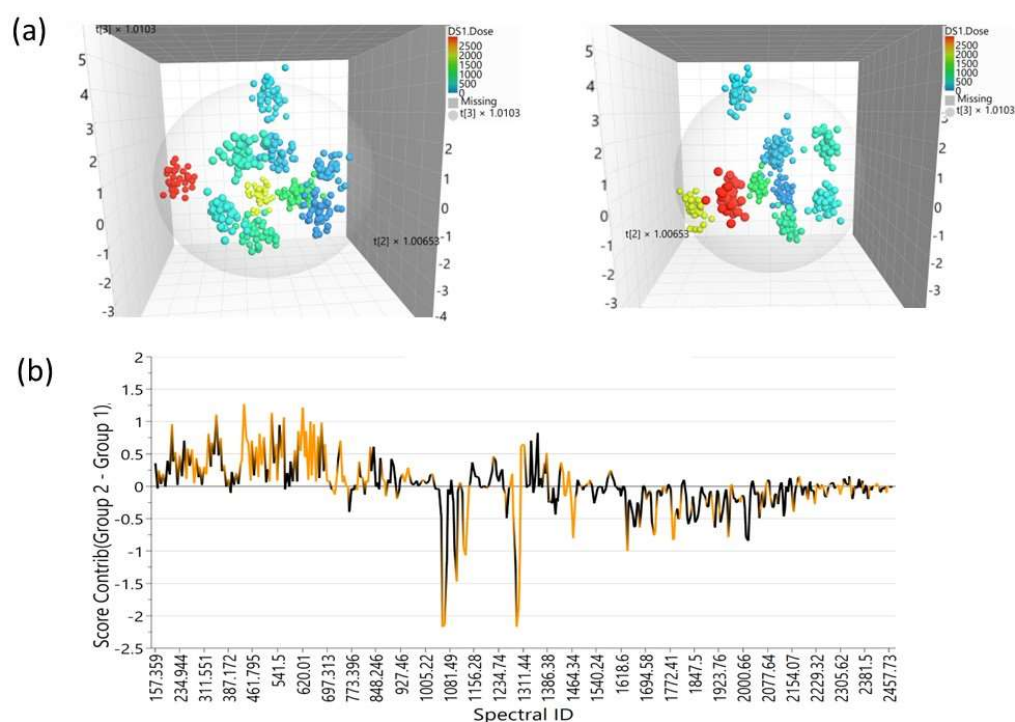


Figure 3. Chemometric analysis of the cocoa liquor produced after irradiating the CCN-51 samples: (a) Front and right-rotated side views of the 3D scatterplot for the scores. The nominal radiation doses were 0.00, 0.10, 0.20, 0.30, 0.45, 0.60, 0.75, 1.00, 2.00, and 3.00 kGy. (b) Contribution plot for the non-irradiated samples (lower/positive side) with respect to the 2.00 kGy irradiated samples (upper/negative side). The orange-colored variables are outside the 3 std dev limit range.

The mild acid taste of CCN-51 was maintained at 0.3 and 0.45 kGy, while it decreased at 0.6 kGy and higher doses. The largest reduction in this attribute occurred at 0.75 kGy, and an increase was observed at 0.2 kGy. The acid taste of the National variety is lower; this behavior was maintained at almost all of the irradiation doses. This attribute increased at 0.1 kGy, but decreased at 0.6 and 1.0, and was completely lost at 3.0 kGy. Acids formed during cocoa fermentation, such as lactic and acetic acids, provide acid notes that constitute a typical flavor attribute [75,79]. Based on experimental data, it can be deduced that the gamma irradiation could decrease the acidity of both varieties at 1.0 kGy and higher doses, and to a greater extent in the CCN-51 variety. The increase in acidity could be due to the degradation of large fat molecules caused by the radiation, which renders the production of smaller ones, including free fatty acids [80]. On the other hand, the reduction in acidity might be a consequence of the hydrolytic decomposition of the acid groups caused by the gamma rays [81].

The behavior of bitter and astringent attributes could be explained by the changes in the contents of antioxidants that may affect the sensory profile of the cocoa liquor prepared from irradiated beans, since plants and plant materials use their antioxidant system as a defense mechanism against the stress caused by products of oxidative reactions, such as the free radicals released through gamma irradiation [82].

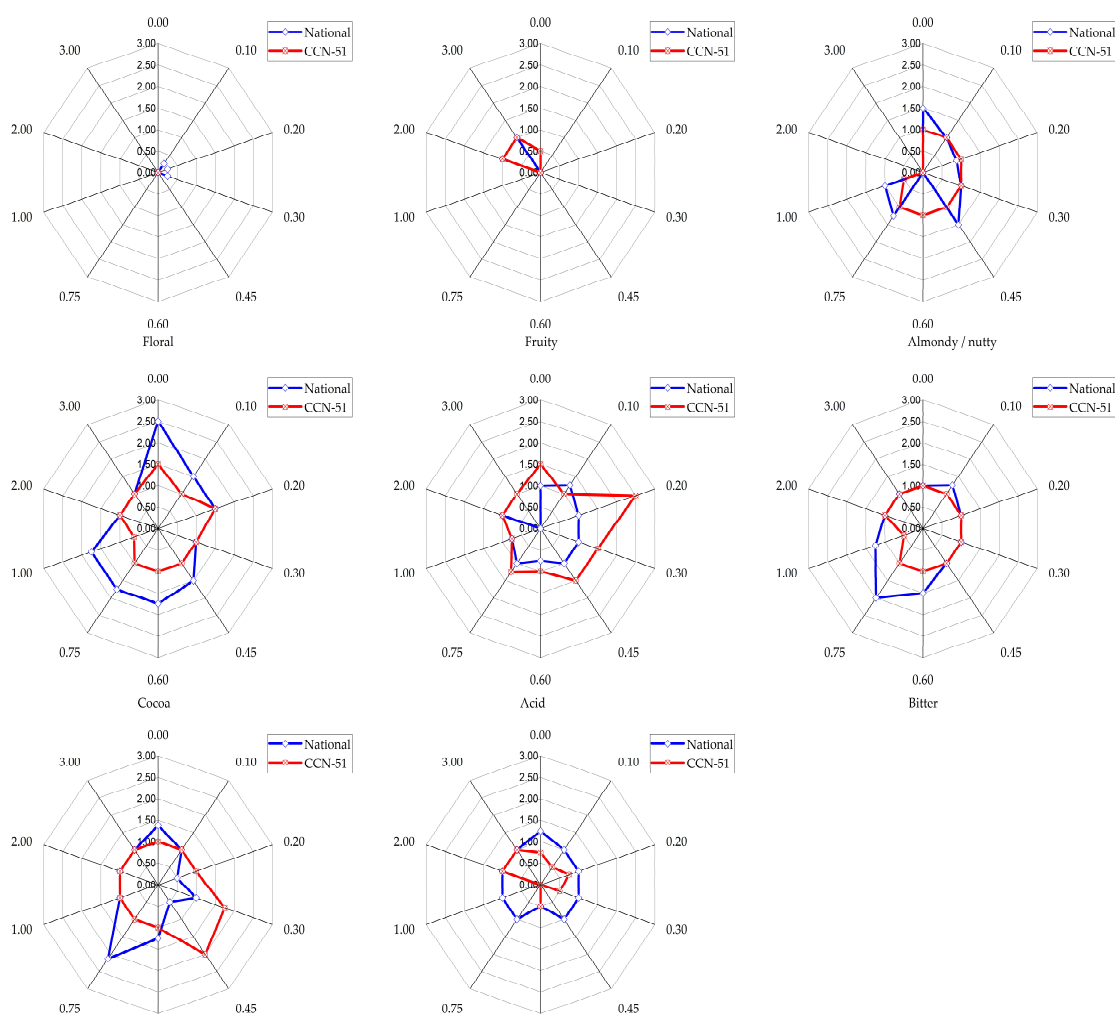


Figure 4. Sensory attributes of the cocoa liquor from the gamma-irradiated cocoa beans. The scales of the attributes are based on the intensity that was generated after the treatments. The radiation treatments are represented in kGy on the radial axis, where 0 corresponds to the control (non-irradiated).

The mild bitter taste determined in the CCN-51 control sample was maintained under the different treatments and decreased only at 1.00 kGy. In contrast, this attribute in the National variety increased at 0.1, 0.6, 0.75, and 1.0 kGy. The most remarkable increment was at 0.75 kGy, which may suggest that radiation also interacts with the compounds responsible for bitter taste. The presence of methylxanthines—namely, theobromine and caffeine—provides the bitter taste that consumers perceive in Amazonian cocoa and chocolate [83]. Indeed, alkaloid and flavonoid contents, antioxidant activity, and phenolic compounds have been found to be increased in gamma-irradiated seeds [84,85]. Moreover, a correlation between total polyphenol content and bitter flavor has been evidenced [86]. This may explain the increasing bitter taste in the cocoa liquor obtained from the irradiated beans. Conversely, a study of gamma-irradiated monsooned coffee suggested that the dose produced an increasing degradation of the chlorogenic acid [87], which may explain the reduction in the bitter taste in the evaluated cocoa liquors.

The astringency in CCN-51 only changed at 0.3 and 0.45 kGy—doses at which the attribute increased. In the National variety, it decreased in all of the treatments, except at 0.75 kGy. The reduction in the cocoa beans' astringency could improve their palatability, since an increase in bitterness, astringency, and acidity (due to inappropriate fermentation) could negatively affect the cocoa flavor and other attributes [74].

The aroma intensity in CCN-51 was completely lost when doses of 0.45, 0.75, and 1.0 kGy were used, but it increased at 2.0 and 3.0 kGy. Unlike what was observed in the bulk variety, the aroma of the National variety cocoa liquor decreased in all of the radiation treatments, with a maximum reduction at 0.6 kGy.

Other authors have also found differences in the flavor profiles of irradiated samples. A study of dried scallions exposed separately to three irradiation sources and subsequently assessed by electronic sensing (e-nose and e-tongue) concluded that the irradiation treatments affected the amounts of the identified volatile compounds. A significant increase associated with the aroma profile was found at 4 and 7 kGy, while the perception of the taste attributes increased at the last dose (7 kGy) for the samples irradiated by an e-beam and with gamma rays. There was a detectable change in the volatile compound profile during the gamma-ray treatment [88]. Kakkugi samples prepared with red pepper powder ionized with gamma rays at doses of 0 (control), 3, 5, and 7 kGy were grouped in four different clusters, after the e-nose analysis at the beginning of the fermentation process. This could have been due to the influence of radiation on the odor molecules [89]. Grapes subjected to gamma irradiation at 0.67, 1.3, 2.0, and 2.7 kGy exhibited increases in their anthocyanin concentrations at higher doses, whilst maintaining their flavanol and flavonol contents. The concentrations of the aromatic compounds associated with the fruity and floral notes showed an increase at the first three doses [90].

The increase in the perception of aroma attributes may be explained by the influence of radiation on the compound bonds. For instance, bounded glycosides in grapevines were identified as odorless, in contrast with free volatile compounds, which showed an impact on the aroma and flavor [90,91]. Moreover, a study on irradiated nutmeg concluded that glycosides responsible for aroma broke down due to the irradiation. Consequently, there was an enhancement in the contents of the nutmeg's volatile compounds [90,92].

Both the CCN-51 and National varieties showed a rancid flavor in the samples irradiated at 1.0 kGy, and it was more intense at 2.0 and 3.0 kGy. This could be attributed to the interaction of the triacylglycerol fatty acids with gamma rays; in particular, unsaturated fatty acids are susceptible to radiation, and they generate products that contribute to rancidity [93].

4. Conclusions

To the best of our knowledge, this study is the first to assess the influence of induced magnetic fields during cocoa beans' fermentation on the constituents of the cocoa liquor obtained from them, as well as the influence of gamma irradiation of fermented cocoa beans on the flavor constituents of the liquor. Raman spectroscopy enables the identification of the main compounds that are present in cocoa liquor. The Raman spectra of cocoa liquor were attributed to lipids, lignocellulosic compounds, pectins, flavonoids, theobromine, and organic acids. Also, the irradiation dose, the electric field intensity, and the cocoa variety could be discriminated using Raman spectra and chemometric tools. Therefore, this study provides evidence for the potential application of this spectroscopic tool to identify and evaluate irradiated foods and fermented products exposed under induced magnetic fields. The cocoa constituents exhibited interactions with gamma rays that could be translated into changes in the sensory profile of the resulting cocoa liquors, which are perceptible to human senses. In this regard, their sensory attributes exhibited varying behaviors depending on the dose, and some of them showed a marked tendency (i.e., rancid) at 1 kGy and higher doses. Indeed, radiation exerts an influence on the cocoa bean constituents and the compounds responsible for the sensory attributes in the cocoa liquor prepared with irradiated National and CCN-51 cocoa beans. The determination of a dose that provides the benefits of irradiation while preserving cocoa's nutritional and flavor attributes should be pursued in future research.

Regarding the fermentation of the cocoa under induced magnetic fields, further experiments are needed to find out and better explain all of the variables responsible for the data dispersion, which would help improve the cocoa liquor processing.

Supplementary Materials: The following supporting information can be downloaded at: <https://www.mdpi.com/article/10.3390/foods12213924/s1>, Figure S1: Schematic representation of the dosimeter location at four positions in the plastic trays, identification of the maximum and minimum dose, and dose uniformity rate (DUR) calculus at each irradiation treatment in the (a) National and (b) CCN-51 varieties. Figure S2: Location of the four dosimeters at positions A, B, C, and D in the plastic tray containing the cocoa beans for each treatment. Table S1: Time treatment, nominal dose, dosimeter readings, and DUR for the irradiated National cocoa beans. Table S2: Time treatment, nominal dose, dosimeter readings, and DUR for the irradiated CCN-51 cocoa beans. Table S3: Averages of the evaluated attributes in the cocoa liquor obtained from fermented and dried beans irradiated at different nominal doses for the CCN-51 and National varieties.

Author Contributions: Conceptualization, J.R., P.V.-J. and L.R.-G.; methodology, T.M.G.-A., C.C.-P., J.B., M.S., A.P. and E.V. (Edison Vera); formal analysis, F.E.O.-O., V.C., L.R.-G. and P.V.-J.; investigation, T.M.G.-A., C.C.-P., J.B., A.E. and A.P.; writing—original draft preparation, T.M.G.-A. and C.C.-P.; writing—review and editing, J.R., E.V. (Edwin Vera), L.R.-G. and P.V.-J. All authors have read and agreed to the published version of the manuscript.

Funding: This research received no external funding.

Data Availability Statement: The data used to support the findings of this study can be made available by the corresponding author upon request.

Acknowledgments: The authors acknowledge to “Programa de Reactivación de Café y Cacao” of Ministerio de Agricultura y Ganadería (Ecuador) for providing the National cocoa samples for this study.

Conflicts of Interest: The authors declare no conflict of interest.

References

1. Sepúlveda, W.S.; Maza, M.T.; Uldemolins, P.; Cantos-Zambrano, E.G.; Ureta, I. Linking dark chocolate product attributes, consumer preferences, and consumer utility: Impact of quality labels, cocoa content, chocolate origin, and price. *J. Int. Food Agribus. Mark.* **2022**, *34*, 518–537. [[CrossRef](#)]
2. Bahari, A.; Akoh, C.C. Texture, rheology and fat bloom study of ‘chocolates’ made from cocoa butter equivalent synthesized from illipe butter and palm mid-fraction. *LWT* **2018**, *97*, 349–354. [[CrossRef](#)]
3. Toker, O.S.; Pirouzian, H.R.; Palabiyik, I.; Konar, N. Chocolate flow behavior: Composition and process effects. *Crit. Rev. Food Sci. Nutr.* **2023**, *63*, 3788–3802. [[CrossRef](#)]
4. Ziegleder, G. Flavour development in cocoa and chocolate. In *Beckett’s Industrial Chocolate Manufacture and Use*, 5th ed.; Beckett, S.T., Fowler, M.S., Ziegler, G.R., Eds.; John Wiley & Sons Ltd.: Chichester, UK, 2017; pp. 185–215.
5. Almeida, O.G.G.; Pinto, U.M.; Matos, C.B.; Frazilio, D.A.; Braga, V.F.; von Zeska-Kress, M.R.; De Martinis, E.C.P. Does Quorum sensing play a role in microbial shifts along spontaneous fermentation of cocoa beans? An in silico perspective. *Food Res. Int.* **2020**, *131*, 109034. [[CrossRef](#)]
6. Gutiérrez-Ríos, H.G.; Suárez-Quiroz, M.L.; Hernández-Estrada, Z.J.; Castellanos-Onorio, O.P.; Alonso-Villegas, R.; Rayas-Duarte, P.; Cano-Sarmiento, C.; Figueroa-Hernández, C.Y.; González-Ríos, O. Yeasts as producers of flavor precursors during cocoa bean fermentation and their Relevance as starter cultures: A review. *Fermentation* **2022**, *8*, 331. [[CrossRef](#)]
7. Guo, L.; Guo, Y.; Wu, P.; Liu, S.; Gu, C.; Yolandan, Wu, M.; Ma, H.; He, R. Enhancement of polypeptide yield derived from rapeseed meal with low-intensity alternating magnetic field. *Foods* **2022**, *11*, 2952. [[CrossRef](#)] [[PubMed](#)]
8. Guzmán-Armenteros, T.M.; Ramos-Guerrero, L.A.; Guerra, L.S.; Weckx, S.; Ruales, J. Optimization of cacao beans fermentation by native species and electromagnetic fields. *Heliyon* **2023**, *9*, e15065. [[CrossRef](#)]
9. Abinaya, S.; Panghal, A.; Roopa, H.; Chhikara, N.; Kumari, A.; Gehlot, R. Utilization of magnetic fields in food industry. In *Novel Technologies in Food Science*; Chhikara, N., Panghal, A., Gaurav, G., Eds.; John Wiley & Sons, Ltd.: Hoboken, NJ, USA, 2023; pp. 171–233.
10. Oberrauter, L.M.; Januszewska, R.; Schlich, P.; Majchrzak, D. Sensory evaluation of dark origin and non-origin chocolates applying Temporal Dominance of Sensations (TDS). *Food Res. Int.* **2018**, *111*, 39–49. [[CrossRef](#)]
11. Del Rio, D.; Rodriguez-Mateos, A.; Spencer, J.P.E.; Tognolini, M.; Borges, G.; Crozier, A. Dietary (poly)phenolics in human health: Structures, bioavailability, and evidence of protective effects against chronic diseases. *Antioxid. Redox Signal.* **2013**, *18*, 1818–1892. [[CrossRef](#)]
12. Żyżelewicz, D.; Bojczuk, M.; Budryn, G.; Zduńczyk, Z.; Juśkiewicz, J.; Jurgoński, A.; Oracz, J. Influence of diet based on bread supplemented with raw and roasted cocoa bean extracts on physiological indices of laboratory rats. *Food Res. Int.* **2018**, *112*, 209–216. [[CrossRef](#)]
13. Inamura, P.Y.; Uehara, V.B.; Teixeira, C.A.H.M.; del Mastro, N.L. Mediate gamma radiation effects on some packaged food items. *Radiat. Phys. Chem.* **2012**, *81*, 1144–1146. [[CrossRef](#)]

14. Farkas, J.; Ehlermann, D.A.E.; Mohácsi-Farkas, C. Food Technologies: Food Irradiation. In *Encyclopedia of Food Safety*, 1st ed.; Motarjemi, Y., Ed.; Elsevier: Amsterdam, Netherlands, 2014; pp. 178–186.
15. Ravindran, R.; Jaiswal, A.K. Wholesomeness and safety aspects of irradiated foods. *Food Chem.* **2019**, *285*, 363–368. [[CrossRef](#)] [[PubMed](#)]
16. Mshelia, R.D.Z.; Dibal, N.I.; Chiroma, S.M. Food irradiation: An effective but under-utilized technique for food preservations. *J. Food Sci. Technol.* **2022**, *60*, 2517–2525. [[CrossRef](#)] [[PubMed](#)]
17. Calado, T.; Venâncio, A.; Abrunhosa, L. Irradiation for mold and mycotoxin control: A review. *Compr. Rev. Food Sci. Food Saf.* **2014**, *13*, 1049–1061. [[CrossRef](#)]
18. Prakash, A. What is the benefit of irradiation compared to other methods of food preservation? In *Genetically Modified and Irradiated Food*, 1st ed.; Andersen, V., Ed.; Elsevier: Amsterdam, The Netherlands, 2020; pp. 217–231.
19. Hallman, G.J. Process control in phytosanitary irradiation of fresh fruits and vegetables as a model for other phytosanitary treatment processes. *Food Control* **2017**, *72*, 372–377. [[CrossRef](#)]
20. Stefanova, R.; Vasilev, N.V.; Spassov, S.L. Irradiation of food, current legislation framework, and detection of irradiated foods. *Food Anal. Methods* **2010**, *3*, 225–252. [[CrossRef](#)]
21. Stewart, E.M. Food irradiation chemistry. In *Food Irradiation: Principles and Applications*; Molins, R.A., Ed.; John Wiley & Sons Inc.: Toronto, ON, Canada, 2001; pp. 37–76.
22. Farkas, J.; Mohácsi-Farkas, C. History and future of food irradiation. *Trends Food Sci. Technol.* **2011**, *22*, 121–126. [[CrossRef](#)]
23. Zhao, L.; Wang, S. Developing treatment protocols for disinfecting pine wood product using radio frequency energy. *Eur. J. Wood Wood Prod.* **2018**, *76*, 191–200. [[CrossRef](#)]
24. Ferrier, P. Irradiation as a quarantine treatment. *Food Policy* **2010**, *35*, 548–555. [[CrossRef](#)]
25. Braga, S.C.G.N.; Oliveira, L.F.; Hashimoto, J.C.; Gama, M.R.; Efraim, P.; Poppi, R.J.; Augusto, F. Study of volatile profile in cocoa nibs, cocoa liquor and chocolate on production process using GC × GC-QMS. *Microchem. J.* **2018**, *141*, 353–361. [[CrossRef](#)]
26. Toker, O.S.; Palabiyik, I.; Konar, N. Chocolate quality and conching. *Trends Food Sci. Technol.* **2019**, *91*, 446–453. [[CrossRef](#)]
27. Hinneh, M.; Abotsi, E.E.; Van de Walle, D.; Tzompa-Sosa, D.A.; De Winne, A.; Simonis, J.; Messens, K.; Van Durme, J.; Afoakwa, E.O.; De Cooman, L.; et al. Pod storage with roasting: A tool to diversifying the flavor profiles of dark chocolates produced from ‘bulk’ cocoa beans? (Part II: Quality and sensory profiling of chocolates). *Food Res. Int.* **2020**, *132*, 109116. [[CrossRef](#)]
28. Belščak-Cvitanović, A.; Komes, D.; Dujmović, M.; Karlović, S.; Biškić, M.; Brnčić, M.; Ježek, D. Physical, bioactive and sensory quality parameters of reduced sugar chocolates formulated with natural sweeteners as sucrose alternatives. *Food Chem.* **2015**, *167*, 61–70. [[CrossRef](#)] [[PubMed](#)]
29. Suzuki, R.M.; Montanher, P.F.; Visentainer, J.V.; de Souza, N.E. Composição centesimal e quantificação de ácidos graxos nas cinco maiores marcas de chocolates do Brasil. *Cienc. Tecnol. Aliment.* **2011**, *31*, 541–546. [[CrossRef](#)]
30. Patel, K.K.; Kar, A.; Jha, S.N.; Khan, M.A. Machine vision system: A tool for quality inspection of food and agricultural products. *J. Food Sci. Technol.* **2012**, *49*, 123–141. [[CrossRef](#)]
31. Nunes, C.A. Vibrational spectroscopy and chemometrics to assess authenticity, adulteration and intrinsic quality parameters of edible oils and fats. *Food Res. Int.* **2014**, *60*, 255–261. [[CrossRef](#)]
32. Vargas Jentzsch, P.; Ciobotă, V.; Salinas, W.; Kampe, B.; Aponte, P.M.; Rösch, P.; Popp, J.; Ramos, L.A. Distinction of ecuadorian varieties of fermented cocoa beans using Raman spectroscopy. *Food Chem.* **2016**, *211*, 274–280. [[CrossRef](#)] [[PubMed](#)]
33. Salvador, L.; Guijarro, M.; Rubio, D.; Aucatoma, B.; Guillén, T.; Vargas Jentzsch, P.; Ciobotă, V.; Stolker, L.; Ulic, S.; Vásquez, L.; et al. Exploratory monitoring of the quality and authenticity of commercial honey in Ecuador. *Foods* **2019**, *8*, 105. [[CrossRef](#)]
34. Vargas Jentzsch, P.; Sandoval Pauker, C.; Zárate Pozo, P.; Sinche Serra, M.; Jácome Camacho, G.; Rueda-Ayala, V.; Garrido, P.; Ramos Guerrero, L.; Ciobotă, V. Raman spectroscopy in the detection of adulterated essential oils: The case of nonvolatile adulterants. *J. Raman Spectrosc.* **2021**, *52*, 1055–1063. [[CrossRef](#)]
35. Vargas Jentzsch, P.; Torrico-Vallejos, S.; Mendieta-Brito, S.; Ramos, L.A.; Ciobotă, V. Detection of counterfeit stevia products using a handheld raman spectrometer. *Vib. Spectrosc.* **2016**, *83*, 126–131. [[CrossRef](#)]
36. Regulla, D. Alanine Dosimetry—A versatile dosimetric tool. In *Proceedings of the World Congress on Medical Physics and Biomedical Engineering, Munich, Germany, 7–12 September 2009; IFMBE Proceedings. Dössel, O., Schlegel, W.C., Eds.; Springer: Berlin, Germany, 2009; Volume 25/3, pp. 478–481.*
37. Bresson, S.; Rousseau, D.; Ghosh, S.; El Marssi, M.; Faivre, V. Raman spectroscopy of the polymorphic forms and liquid state of cocoa butter. *Eur. J. Lipid Sci. Technol.* **2011**, *113*, 992–1004. [[CrossRef](#)]
38. Papalexandratou, Z.; Kaasik, K.; Kauffmann, L.V.; Skorstengaard, A.; Bouillon, G.; Espensen, J.L.; Hansen, L.H.; Jakobsen, R.R.; Blennow, A.; Krych, L.; et al. Linking cocoa varieties and microbial diversity of nicaraguan fine cocoa bean fermentations and their impact on final cocoa quality appreciation. *Int. J. Food Microbiol.* **2019**, *304*, 106–118. [[CrossRef](#)] [[PubMed](#)]
39. Torres-Moreno, M.; Torrescasana, E.; Salas-Salvadó, J.; Blanch, C. Nutritional composition and fatty acids profile in cocoa beans and chocolates with different geographical origin and processing conditions. *Food Chem.* **2015**, *166*, 125–132. [[CrossRef](#)] [[PubMed](#)]
40. Lipp, M.; Anklam, E. Review of cocoa butter and alternative fats for use in chocolate—Part A. Compositional data. *Food Chem.* **1998**, *62*, 73–97. [[CrossRef](#)]
41. Ghazani, S.M.; Marangoni, A.G. Molecular origins of polymorphism in cocoa butter. *Annu. Rev. Food Sci. Technol.* **2021**, *12*, 567–590. [[CrossRef](#)]

42. Saldaña, M.D.A.; Mohamed, R.S.; Mazzafera, P. Extraction of cocoa butter from Brazilian cocoa beans using supercritical CO₂ and ethane. *Fluid Phase Equilib.* **2002**, *194–197*, 885–894. [[CrossRef](#)]
43. Mohamed, I.O. Enzymatic synthesis of cocoa butter equivalent from olive oil and palmitic-stearic fatty acid mixture. *Appl. Biochem. Biotechnol.* **2015**, *175*, 757–769. [[CrossRef](#)]
44. Jahurul, M.H.A.; Zaidul, I.S.M.; Norulaini, N.A.N.; Sahena, F.; Jinap, S.; Azmir, J.; Sharif, K.M.; Mohd Omar, A.K. Cocoa butter fats and possibilities of substitution in food products concerning cocoa varieties, alternative sources, extraction methods, composition, and characteristics. *J. Food Eng.* **2013**, *117*, 467–476. [[CrossRef](#)]
45. Bresson, S.; Lecuelle, A.; Bougrioua, F.; El Hadri, M.; Baeten, V.; Courty, M.; Pilard, S.; Rigaud, S.; Faivre, V. Comparative structural and vibrational investigations between cocoa butter (cb) and cocoa butter equivalent (CBE) by ESI/MALDI-HRMS, XRD, DSC, MIR and Raman spectroscopy. *Food Chem.* **2021**, *363*, 130319. [[CrossRef](#)]
46. Kobayashi, M. Crystallization and polymorphism of fats and fatty acids. In *Vibrational Spectroscopic Aspects of Polymorphism and Phase Transition of Fats and Fatty Acids*; Garty, N., Sato, K., Eds.; Marcel Dekker Inc.: New York, NY, USA, 1988; pp. 139–187.
47. Bresson, S.; El Marssi, M.; Khelifa, B. Raman spectroscopy investigation of various saturated monoacid triglycerides. *Chem. Phys. Lipids* **2005**, *134*, 119–129. [[CrossRef](#)]
48. Czamara, K.; Majzner, K.; Pacia, M.Z.; Kochan, K.; Kaczor, A.; Baranska, M. Raman spectroscopy of lipids: A review. *J. Raman Spectrosc.* **2015**, *46*, 4–20. [[CrossRef](#)]
49. De Gelder, J.; De Gussem, K.; Vandenabeele, P.; Moens, L. Reference database of Raman spectra of biological molecules. *J. Raman Spectrosc.* **2007**, *38*, 1133–1147. [[CrossRef](#)]
50. Edwards, H.G.M.; Villar, S.E.J.; de Oliveira, L.F.C.; Le Hyaric, M. Analytical Raman spectroscopic study of cacao seeds and their chemical extracts. *Anal. Chim. Acta* **2005**, *538*, 175–180. [[CrossRef](#)]
51. Bresson, S.; El Marssi, M.; Khelifa, B. Conformational influences of the polymorphic forms on the CO and C-H stretching modes of five saturated monoacid triglycerides studied by Raman spectroscopy at various temperatures. *Vib. Spectrosc.* **2006**, *40*, 263–269. [[CrossRef](#)]
52. Castro-Alayo, E.M.; Torrejón-Valqui, L.; Cayo-Colca, I.S.; Cárdenas-Toro, F.P. Evaluation of the miscibility of novel cocoa butter equivalents by Raman mapping and multivariate curve resolution–alternating least squares. *Foods* **2021**, *10*, 3101. [[CrossRef](#)] [[PubMed](#)]
53. Agarwal, U.P.; Ralph, S.A. FT-Raman spectroscopy of wood: Identifying contributions of lignin and carbohydrate polymers in the spectrum of black spruce (*Picea mariana*). *Appl. Spectrosc.* **1997**, *51*, 1648–1655. [[CrossRef](#)]
54. Agarwal, U.P.; McSweeney, J.D.; Ralph, S.A. FT-Raman investigation of milled-wood lignins: Softwood, hardwood, and chemically modified black spruce lignins. *J. Wood Chem. Technol.* **2011**, *31*, 324–344. [[CrossRef](#)]
55. Agarwal, U.P. An Overview of Raman spectroscopy as applied to lignocellulosic materials. In *Advances in Lignocellulosics Characterization*; Arguyropoulos, D.S., Ed.; TAPPI Press: Atlanta, GA, USA, 1999; pp. 201–225.
56. Schenzel, K.; Fischer, S. NIR FT Raman spectroscopy—A rapid analytical tool for detecting the transformation of cellulose polymorphs. *Cellulose* **2001**, *8*, 49–57. [[CrossRef](#)]
57. Blackwell, J.; Vasko, P.D.; Koenig, J.L. Infrared and Raman spectra of the cellulose from the cell wall of *Valonia ventricosa*. *J. Appl. Phys.* **1970**, *41*, 4375–4379. [[CrossRef](#)]
58. Yapo, B.M. Pectic substances: From simple pectic polysaccharides to complex pectins—A new hypothetical model. *Carbohydr. Polym.* **2011**, *86*, 373–385. [[CrossRef](#)]
59. Synytsya, A.; Čopíková, J.; Matějka, P.; Machovič, V. Fourier transform Raman and infrared spectroscopy of pectins. *Carbohydr. Polym.* **2003**, *54*, 97–106. [[CrossRef](#)]
60. Gottumukkala, R.V.S.S.; Nadimpalli, N.; Sukala, K.; Subbaraju, G.V. Determination of catechin and epicatechin content in chocolates by high-performance liquid chromatography. *Int. Sch. Res. Not.* **2014**, *2014*, 628196. [[CrossRef](#)] [[PubMed](#)]
61. Colthup, N.; Daly, L.; Wiberley, S. *Introduction to Infrared and Raman Spectroscopy*; Academic Press: San Diego, CA, USA, 1990.
62. Bicchieri, M.; Monti, M.; Piantanida, G.; Sodo, A. Non-destructive spectroscopic investigation on historic Yemenite scriptorial fragments: Evidence of different degradation and recipes for iron tannic inks. *Anal. Bioanal. Chem.* **2013**, *405*, 2713–2721. [[CrossRef](#)] [[PubMed](#)]
63. Mazurek, S.; Fecka, I.; Węglińska, M.; Szostak, R. Quantification of active ingredients in *Potentilla tormentilla* by Raman and infrared spectroscopy. *Talanta* **2018**, *189*, 308–314. [[CrossRef](#)]
64. Aprotosoai, A.C.; Luca, S.V.; Miron, A. Flavor chemistry of cocoa and cocoa products—An overview. *Compr. Rev. Food Sci. Food Saf.* **2016**, *15*, 73–91. [[CrossRef](#)] [[PubMed](#)]
65. Tuenter, E.; Delbaere, C.; De Winne, A.; Bijttebier, S.; Custers, D.; Foubert, K.; Van Durme, J.; Messens, K.; Dewettinck, K.; Pieters, L. Non-volatile and volatile composition of West African bulk and Ecuadorian fine-flavor cocoa liquor and chocolate. *Food Res. Int.* **2020**, *130*, 108943. [[CrossRef](#)]
66. Tuenter, E.; Foubert, K.; Pieters, L. Mood components in cocoa and chocolate: The mood pyramid. *Planta Med.* **2018**, *84*, 839–844. [[CrossRef](#)]
67. Xia, J.; Wang, D.; Liang, P.; Zhang, D.; Du, X.; Ni, D.; Yu, Z. Vibrational (FT-IR, Raman) analysis of tea catechins based on both theoretical calculations and experiments. *Biophys. Chem.* **2020**, *256*, 106282. [[CrossRef](#)]

68. Edwards, H.G.M.; Munshi, T.; Anstis, M. Raman Spectroscopic Characterisations and analytical discrimination between caffeine and demethylated analogues of pharmaceutical relevance. *Spectrochim. Acta Part A Mol. Biomol. Spectrosc.* **2005**, *61*, 1453–1459. [[CrossRef](#)]
69. Gunasekaran, S.; Sankari, G.; Ponnusamy, S. Vibrational spectral investigation on xanthine and its derivatives—Theophylline, caffeine and theobromine. *Spectrochim. Acta Part A Mol. Biomol. Spectrosc.* **2005**, *61*, 117–127. [[CrossRef](#)]
70. Luna, F.; Crouzillat, D.; Cirou, L.; Bucheli, P. Chemical composition and flavor of Ecuadorian cocoa liquor. *J. Agric. Food Chem.* **2002**, *50*, 3527–3532. [[CrossRef](#)]
71. Jehlička, J.; Vitek, P.; Edwards, H.G.M. Raman spectra of organic acids obtained using a portable instrument at $-5\text{ }^{\circ}\text{C}$ in a mountain area at 2000 m above sea level. *J. Raman Spectrosc.* **2010**, *41*, 440–444.
72. Panicker, C.Y.; Varghese, H.T.; Philip, D. FT-IR, FT-Raman and SERS spectra of vitamin C. *Spectrochim. Acta Part A Mol. Biomol. Spectrosc.* **2006**, *65*, 802–804. [[CrossRef](#)] [[PubMed](#)]
73. Rottiers, H.; Tzompa Sosa, D.A.; De Winne, A.; Ruales, J.; De Clippeleer, J.; De Leersnyder, I.; De Wever, J.; Everaert, H.; Messens, K.; Dewettinck, K. Dynamics of volatile compounds and flavor precursors during spontaneous fermentation of fine flavor trinitario cocoa beans. *Eur. Food Res. Technol.* **2019**, *245*, 1917–1937. [[CrossRef](#)]
74. Vera Chang, J.F.; Vallejo Torres, C.; Párraga Morán, D.E.; Macías Véliz, J.; Ramos Remache, R.; Morales Rodríguez, W. Atributos físicos-químicos y sensoriales de las almendras de quince clones de cacao Nacional (*Theobroma cacao* L.) en el Ecuador. *Cienc. Tecnol.* **2015**, *7*, 21–34. [[CrossRef](#)]
75. Kadow, D.; Bohlmann, J.; Phillips, W.; Lieberei, R. Identification of main fine or flavour components in two genotypes of the cocoa tree (*Theobroma cacao* L.). *J. Appl. Bot. Food Qual.* **2013**, *86*, 90–98.
76. Liu, M.; Liu, J.; He, C.; Song, H.; Liu, Y.; Zhang, Y.; Wang, Y.; Guo, J.; Yang, H.; Su, X. Characterization and comparison of key aroma-active compounds of cocoa liquors from five different areas. *Int. J. Food Prop.* **2017**, *20*, 2396–2408. [[CrossRef](#)]
77. Criollo Nuñez, J.; Ramirez-Toro, C.; Bolivar, G.; Sandoval A, A.P.; Lozano Tovar, M.D. Effect of microencapsulated inoculum of *Pichia kudriavzevii* on the fermentation and sensory quality of cacao CCN51 genotype. *J. Sci. Food Agric.* **2023**, *103*, 2425–2435. [[CrossRef](#)]
78. Chang, A.C. The effects of gamma irradiation on rice wine maturation. *Food Chem.* **2003**, *83*, 323–327. [[CrossRef](#)]
79. Krähmer, A.; Engel, A.; Kadow, D.; Ali, N.; Umaharan, P.; Kroh, L.W.; Schulz, H. Fast and neat—Determination of biochemical quality parameters in cocoa using near infrared spectroscopy. *Food Chem.* **2015**, *181*, 152–159. [[CrossRef](#)]
80. Zhang, Z.; Xie, Q.; Che, L. Effects of gamma irradiation on aflatoxin B₁ levels in soybean and on the properties of soybean and soybean oil. *Appl. Radiat. Isot.* **2018**, *139*, 224–230. [[CrossRef](#)]
81. Samra, S.E.; Youssef, A.M.; Ahmed, A.I. Effect of gamma irradiation on the surface and catalytic properties of Al₂O₃ and NiO-Al₂O₃ catalysts. *Bull. Soc. Chim. Fr.* **1990**, *127*, 174–178.
82. Kiani, D.; Borzouei, A.; Ramezani, S.; Soltanloo, H.; Saadati, S. Application of gamma irradiation on morphological, biochemical, and molecular aspects of wheat (*Triticum aestivum* L.) under different seed moisture contents. *Sci. Rep.* **2022**, *12*, 11082. [[CrossRef](#)] [[PubMed](#)]
83. Gomes Júnior, P.C.; Bezerra dos Santos, V.; Santos Lopes, A.; Iúdice de Souza, J.P.; Souza Pina, J.R.; Albuquerque Chagas Júnior, G.C.; Santana Barboza Marinho, P. Determination of theobromine and caffeine in fermented and unfermented Amazonian cocoa (*Theobroma cacao* L.) beans using square wave voltammetry after chromatographic separation. *Food Control* **2020**, *108*, 106887. [[CrossRef](#)]
84. Mohajer, S.; Mat Taha, R.; Lay, M.M.; Khorasani Esmaeili, A.; Khalili, M. Stimulatory effects of gamma irradiation on phytochemical properties, mitotic behaviour, and nutritional composition of sainfoin (*Onobrychis viciifolia* Scop.). *Sci. World J.* **2014**, *2014*, 854093. [[CrossRef](#)]
85. Aly, A.A.; Maraei, R.W.; Sharafeldin, R.G.; Safwat, G. Yield traits of red radish seeds obtained from plants produced from γ -irradiated seeds and their oil characteristics. *Gesunde Pflanz.* **2023**, *75*, 2089–2099. [[CrossRef](#)]
86. Porras Barrientos, L.D.; Torres Oquendo, J.D.; Gil Garzón, M.A.; Martínez Álvarez, O.L. Effect of the solar drying process on the sensory and chemical quality of cocoa (*Theobroma cacao* L.) cultivated in Antioquia, Colombia. *Food Res. Int.* **2019**, *115*, 259–267. [[CrossRef](#)]
87. Hussain, P.R.; Chatterjee, S.; Variyar, P.S.; Sharma, A.; Dar, M.A.; Wani, A.M. Bioactive compounds and antioxidant activity of gamma irradiated sun dried apricots (*Prunus armeniaca* L.). *J. Food Compos. Anal.* **2013**, *30*, 59–66. [[CrossRef](#)]
88. Chung, N.; Ramakrishnan, S.R.; Kwon, J.-H. Experimental validation and evaluation of electronic sensing techniques for rapid discrimination of electron-beam, γ -ray, and X-ray irradiated dried green onions (*Allium fistulosum*). *J. Food Sci. Technol.* **2019**, *56*, 5454–5464. [[CrossRef](#)]
89. Lee, J.H.; Lee, K.-T.; Kim, M.R. Effect of gamma-irradiated red pepper powder on the chemical and volatile characteristics of kakkugi, a Korean traditional fermented radish kimchi. *J. Food Sci.* **2005**, *70*, c441–c447. [[CrossRef](#)]
90. Žulj, M.M.; Bandić, L.M.; Bujak, I.T.; Puhelek, I.; Jeromel, A.; Mihajević, B. Gamma irradiation as pre-fermentative method for improving wine quality. *LWT* **2019**, *101*, 175–182. [[CrossRef](#)]
91. Garrido, J.; Borges, F. Wine and grape polyphenols—A chemical perspective. *Food Res. Int.* **2013**, *54*, 1844–1858. [[CrossRef](#)]

92. Ananthakumar, A.; Variyar, P.S.; Sharma, A. Estimation of aroma glycosides of nutmeg and their changes during radiation processing. *J. Chromatogr. A* **2006**, *1108*, 252–257. [[CrossRef](#)] [[PubMed](#)]
93. Ehlermann, D.A.E. Safety of food and beverages: Safety of irradiated foods. In *Encyclopedia of Food Safety*; Motarjemi, Y., Ed.; Elsevier: San Diego, CA, USA, 2014; Volume 3, pp. 447–452.

Disclaimer/Publisher’s Note: The statements, opinions and data contained in all publications are solely those of the individual author(s) and contributor(s) and not of MDPI and/or the editor(s). MDPI and/or the editor(s) disclaim responsibility for any injury to people or property resulting from any ideas, methods, instructions or products referred to in the content.